Can we use satellites to calibrate airborne lidar?

James H. Churnside
NOAA Earth System Research Laboratory (ESRL) Chemical Sciences Division, 325 Broadway, Boulder, CO 80305, USA, james.h.churnside@noaa.gov
Richard D. Marchbanks
University of Colorado Cooperative Institute for Research in Environmental Sciences (CIRES) at the NOAA Earth System Research Laboratory (ESRL) Chemical Sciences Division, 325 Broadway, Boulder, CO 80305, USA, richard.marchbanks@noaa.gov

Abstract: The backscattering coefficient of seawater, defined as the coefficient of scattering at angles > 90 degrees, includes contributions from water and from any particles in the water. The water contribution has a relatively narrow range of values in the ocean, but the particulate contribution depends on the number of particles in the water and their type. Measurements of the particulate backscattering coefficient generally take advantage of the relatively small variability in scattering with angle at angles > 90 degrees to obtain an estimate of the backscattering coefficient from scattering at a single angle. Lidar has been used to infer the backscattering coefficient from scattering at 180 degrees, but this depends on knowledge of the relationship between scattering at this angle and the backscattering coefficient. It also depends on an absolute radiometric calibration, although this can be avoided using high-spectral-resolution lidar. Here, we consider a technique to obtain the backscattering coefficient directly from lidar data by calibration against passive ocean color measurements. The technique does not depend on retrieval of either the lidar calibration coefficient or the relationship between the volume scattering function at 180 degrees and the backscattering coefficient, but can be used to infer both quantities. The only requirement is that the relationship between the scattering parameters not change significantly over the area, depth range, or duration of the measurements. Once the relationship is found, it can be used where the satellite measurements are affected by clouds or vertical structure in the scattering.

1. Introduction

The backscattering coefficient of seawater is defined as the coefficient of scattering at angles > 90°. This includes contributions from water and from any particles in the water. The contribution from water depends slightly on water temperature and salinity [*Shifrin*, 1988], but it has a narrow range of values in the ocean. The contribution from particles depends on the type of particles in the ocean and their number density and has a much larger range of values. The particulate backscatter is important for remote sensing applications because of its relationship to chlorophyll concentration [*Brewin et al.*, 2012; *Huot et al.*, 2008], the concentration of particulate organic carbon [*Stramski et al.*, 1999; *Stramski et al.*, 2008], the carbon content of phytoplankton [*Behrenfeld et al.*, 2005; *Graff et al.*, 2015; *Martinez-Vicente et al.*, 2013], and the total amount of particulate matter [*Boss et al.*, 2004; *Boss et al.*, 2009].

The angular dependence of particulate scattering at angles > 90° is remarkably similar across a wide variety of ocean waters, especially at scattering angles near 120° [*Berthon et al.*, 2007; *Boss and Pegau*, 2001; *Sullivan and Twardowski*, 2009; *Zhang et al.*, 2014]. This feature has been exploited by *in situ* instruments that infer particulate backscattering coefficient from scattering measurements at a single angle near 120°. This feature of oceanic scattering is the justification for neglecting the effects of sun angle to infer backscattering coefficient from

passive instruments in space [*Gordon et al.*, 1988; *Maritorena et al.*, 2002; *Morel and Prieur*, 1977]. More recently, this feature has been applied to airborne [*Churnside et al.*, 2017; *Hair et al.*, 2016; *Schulien et al.*, 2017] and space-based [*Behrenfeld et al.*, 2013; *Lu et al.*, 2014; *Lu et al.*, 2016] lidar, which measures scattering at 180°.

This paper describes a method to infer the backscattering coefficient from oceanographic lidar data using a calibration with passive ocean color measurements. In this method, we do not need to know the radiometric calibration factor of the lidar of the precise relationship between the volume scattering function at 180° and the backscattering coefficient. Instead, both quantities can be inferred from the method.

2. Theory

We will consider the photocathode current in the detector as the primary lidar signal. If the optical properties of the ocean are constant over the measurement depth range of a lidar, this signal is given by [*Churnside*, 2008]

$$I(z) = A\left[\beta_p(\pi) + \beta_w(\pi)\right]\exp(-2\alpha z), \tag{1}$$

where z is depth, A is a calibration factor, β_p is the volume scattering function of particulate scattering, β_w is the volume scattering function of scattering from seawater, and α is the lidar attenuation coefficient. We derive α from a linear fit to the logarithm of the signal, and correct the signal for the effects of attenuation to get

$$I = A\left[\beta_p(\pi) + \beta_w(\pi)\right]. \tag{2}$$

The quality of the fit can be used as an indicator of whether or not the assumption of a uniform profile of the optical properties of the water quality is justified.

The volume scattering function of seawater was taken to be $\beta_w(\pi) = 2.70\times10^{-4}$ m^{-1} sr^{-1}, based on the conditions over the study area [*Mobley*, 1994]. The particulate volume scattering function is related to the particulate backscattering coefficient, b_{bp}, by

$$\beta_p(\pi) = \frac{b_{bp}}{2\pi\chi(\pi)}, \tag{3}$$

where χ is related to the shape of the particulate phase function for scattering angles > 90°. Therefore, we can express the lidar signal as

$$I = \frac{A}{2\pi\chi(\pi)} b_{bp} + 2.70\times10^{-4} A. \tag{4}$$

3. Methods

For b_{bp}, we used the total backscattering at 531 nm from the Moderate Resolution Imaging Spectroradiometer (MODIS) instruments on the Aqua and Terra satellites. The Level 3 data at 4 km resolution were produced using the Generalized Inherent Optical Properties (GIOP) model [*Werdell et al.*, 2013]. At the position of each lidar position, we identified Aqua and Terra MODIS pixels at that position on the day of the lidar flight, the day before and, the day after. We averaged any valid backscattering values within these six satellite images, and did not use lidar profiles with no satellite matches.

We collected lidar data on ten days during the period July 8-20, 2015 off the west coast of Florida (Fig. 1). The lidar configuration for these measurements has been described previously

[*Churnside et al.*, 2017; *Churnside and Marchbanks*, 2017], but we processed the data slightly differently for this analysis. We selected every 25th lidar pulse in order to reduce the correlation between samples in the analysis. We converted digitization level into photocathode current using the known characteristics of the digitizer, logamp, and photomultiplier gain section. We identified the sea surface from the return, and performed a regression on the logarithm of the signal between depths of 2-10 m. We took the exponential of the intercept of that regression as the signal for that lidar pulse. To ensure that the optical properties of the water column were uniform for the data set, we removed lidar data where the standard deviation of the estimate of the intercept of the signal was $\sigma > 0.02$, which corresponds to an uncertainty of 2% in our estimate of the lidar signal.

3. Results

We selected a total of 35,192 data points for analysis using the criteria described above, and these are plotted in Fig. 2. The coefficient of determination, $R^2 = 0.68$. Using an ordinary regression, the best fit, plotted as a dashed line in Fig. 2, was

$$I = 142 \pm 1\ \mu\text{A m}\, b_{bp} + 0.393 \pm 0.003\ \mu\text{A}, \tag{5}$$

where the uncertainties in the parameters represent one standard deviation of the estimate. From the offset, we derived a calibration factor of $A = 1460$ μA m, and, from this value and the slope of the equation, we inferred a shape parameter of $\chi = 1.63$. The root-mean-square error in b_{bp} inferred using this equation was 0.0020 m^{-1}. Where there is random variability in both variables, the Reduced Major Axis (RMA) regression may be more appropriate. The best fit for this regression, plotted as a solid line in Fig. 2, was

$$I = 173 \pm 2\ \mu\text{A m}\, b_{bp} + 0.301 \pm 0.005\ \mu\text{A}. \tag{6}$$

From these values, we inferred a calibration factor of $A = 1110$ μA m and a shape parameter of $\chi = 1.03$. The root-mean-square error in b_{bp} inferred using this equation was 0.0017 m^{-1}.

There are few estimates of the shape parameter at 180°, but there have been measurements at 170°. These include values of $\chi = 0.62 \pm 0.22$ at a coastal site in the NW Atlantic [*Boss and Pegau*, 2001], $\chi = 0.69 \pm 0.08$ at a coastal site in the Black Sea [*Chami et al.*, 2006], and $\chi = 1.09 \pm 0.06$ at ten sites at coastal and open ocean locations [*Sullivan and Twardowski*, 2009]. The value we obtained from the ordinary regression is somewhat higher than we would expect from these measurements, but the RMA result is within the range of measured values. The RMA result is, however, still higher than the value of 0.5 that was used in a previous lidar study [*Hair et al.*, 2016].

4. Conclusions

We conclude that we can use satellites to calibrate airborne lidar. Specifically, we can use passive ocean color measurements of backscattering coefficient to calibrate lidar data and derive the backscattering coefficient from lidar data. We obtained a local relationship between the lidar signal and the particulate backscattering coefficient for the eastern Gulf of Mexico, with a coefficient of determination of $R^2 = 0.68$. From this relationship, we derived the lidar calibration coefficient and the ratio of volume scattering function to backscattering coefficient. We recommend a reduced major axis regression rather than an ordinary regression. Using this regression, we obtained a value for χ that was more consistent with previous measurements and a lower rms error between the inferred and satellite measurements of backscattering coefficient.

Future work will include a comparison of the calibration coefficient obtained by this method with a calculation using the lidar equation [*Churnside*, 2014] and laboratory measurements of system parameters. We also intend to apply the technique to lidar measurements in the Arctic Ocean, where passive ocean color measurements are difficult, and lidar has been suggested as a way to fill in the gaps [*Behrenfeld et al.*, 2016; *Churnside and Marchbanks*, 2015; *Hill and Zimmerman*, 2010].

Acknowledgments

MODIS data were obtained from the NASA Goddard Space Flight Center, Ocean Biology Processing Group; (2017): Moderate Resolution Imaging Spectroradiometer (MODIS) Ocean Color Data, NASA OB.DAAC, Greenbelt, MD, USA. Accessed 2017/10/13.

References

Behrenfeld, M. J., E. Boss, D. A. Siegel, and D. M. Shea (2005), Carbon-based ocean productivity and phytoplankton physiology from space, Global Biogeochemical Cycles, *19*(1), GB1006. doi:10.1029/2004GB002299

Behrenfeld, M. J., Y. Hu, C. A. Hostetler, G. Dall'Olmo, S. D. Rodier, J. W. Hair, and C. R. Trepte (2013), Space-based lidar measurements of global ocean carbon stocks, Geophys. Res. Lett., *40*(16), 4355-4360.

Behrenfeld, M. J., et al. (2016), Annual boom–bust cycles of polar phytoplankton biomass revealed by space-based lidar, Nature Geoscience, *10*, 118. doi:10.1038/ngeo2861

Berthon, J.-F., E. Shybanov, M. E. G. Lee, and G. Zibordi (2007), Measurements and modeling of the volume scattering function in the coastal northern Adriatic Sea, Appl. Opt., *46*(22), 5189-5203. doi:10.1364/AO.46.005189

Boss, E., and W. S. Pegau (2001), Relationship of light scattering at an angle in the backward direction to the backscattering coefficient, Appl. Opt., *40*(30), 5503-5507. doi:10.1364/AO.40.005503

Boss, E., D. Stramski, T. Bergmann, W. S. Pegau, and M. Lewis (2004), Why Should We Measure the Optical Backscattering Coefficient? , Oceanography, *17*(2), 44-49. doi:doi.org/10.5670/oceanog.2004.46

Boss, E., et al. (2009), Comparison of inherent optical properties as a surrogate for particulate matter concentration in coastal waters, Limnol. Oceanogr. Methods, *7*(11), 803-810. doi:10.4319/lom.2009.7.803

Brewin, R. J. W., G. Dall'Olmo, S. Sathyendranath, and N. J. Hardman-Mountford (2012), Particle backscattering as a function of chlorophyll and phytoplankton size structure in the open-ocean, Opt. Express, *20*(16), 17632-17652. doi:10.1364/OE.20.017632

Chami, M., E. Marken, J. J. Stamnes, G. Khomenko, and G. Korotaev (2006), Variability of the relationship between the particulate backscattering coefficient and the volume scattering function measured at fixed angles, J. Geophys. Res. Oceans, *111*(C5), C05013. doi:10.1029/2005JC003230

Churnside, J., R. Marchbanks, C. Lembke, and J. Beckler (2017), Optical Backscattering Measured by Airborne Lidar and Underwater Glider, Remote Sensing, *9*(4), 379

Churnside, J. H. (2008), Polarization effects on oceanographic lidar, Opt. Express, *16*(2), 1196-1207. doi:10.1364/oe.16.001196

Churnside, J. H. (2014), Review of profiling oceanographic lidar, Opt. Eng., *53*(5), 051405. doi:10.1117/1.oe.53.5.051405

Churnside, J. H., and R. Marchbanks (2015), Sub-surface plankton layers in the Arctic Ocean, Geophys. Res. Lett., *42*, 4896-4902. doi:10.1002/2015GL064503

Churnside, J. H., and R. D. Marchbanks (2017), Inversion of oceanographic profiling lidars by a perturbation to a linear regression, Appl. Opt., *56*(18), 5228-5233. doi:10.1364/AO.56.005228

Gordon, H. R., O. B. Brown, R. H. Evans, J. W. Brown, R. C. Smith, K. S. Baker, and D. K. Clark (1988), A semianalytic radiance model of ocean color, J. Geophys. Res. Atmos., *93*(D9), 10909-10924. doi:10.1029/JD093iD09p10909

Graff, J. R., T. K. Westberry, A. J. Milligan, M. B. Brown, G. Dall'Olmo, V. v. Dongen-Vogels, K. M. Reifel, and M. J. Behrenfeld (2015), Analytical phytoplankton carbon measurements spanning diverse ecosystems, Deep Sea Res. I, *102*, 16-25. doi:http://dx.doi.org/10.1016/j.dsr.2015.04.006

Hair, J., et al. (2016), Combined Atmospheric and Ocean Profiling from an Airborne High Spectral Resolution Lidar, EPJ Web of Conferences, *119*, 22001.

Hill, V. J., and R. C. Zimmerman (2010), Estimates of primary production by remote sensing in the Arctic Ocean: Assessment of accuracy with passive and active sensors, Deep Sea Res. I, *57*(10), 1243-1254. doi:10.1016/j.dsr.2010.06.011

Huot, Y., A. Morel, M. S. Twardowski, D. Stramski, and R. A. Reynolds (2008), Particle optical backscattering along a chlorophyll gradient in the upper layer of the eastern South Pacific Ocean, Biogeosciences, *5*(2), 495-507. doi:10.5194/bg-5-495-2008

Lu, X., Y. Hu, C. Trepte, S. Zeng, and J. H. Churnside (2014), Ocean subsurface studies with the CALIPSO spaceborne lidar, J. Geophys. Res. Oceans, *119*(7), 4305-4317. doi:10.1002/2014jc009970

Lu, X., et al. (2016), Retrieval of ocean subsurface particulate backscattering coefficient from space-borne CALIOP lidar measurements, Opt. Express, *24*(25), 29001-29008. doi:10.1364/OE.24.029001

Maritorena, S., D. A. Siegel, and A. R. Peterson (2002), Optimization of a semianalytical ocean color model for global-scale applications, Appl. Opt., *41*(15), 2705-2714. doi:10.1364/ao.41.002705

Martinez-Vicente, V., G. Dall'Olmo, G. Tarran, E. Boss, and S. Sathyendranath (2013), Optical backscattering is correlated with phytoplankton carbon across the Atlantic Ocean, Geophys. Res. Lett., *40*(6), 1154-1158. doi:10.1002/grl.50252

Mobley, C. D. (1994), *Light and Water: Radiative transfer in natural waters*, 592 pp., Academic Press, San Diego.

Morel, A., and L. Prieur (1977), Analysis of variations in ocean color, Limnol. Oceanogr., *22*(4), 709-722.

Schulien, J. A., M. J. Behrenfeld, J. W. Hair, C. A. Hostetler, and M. S. Twardowski (2017), Vertically- resolved phytoplankton carbon and net primary production from a high spectral resolution lidar, Opt. Express, *25*(12), 13577-13587. doi:10.1364/OE.25.013577

Shifrin, K. S. (1988), *Physical Optics of Ocean Water*, 285 pp., American Institute of Physics, New York.

Stramski, D., R. A. Reynolds, M. Kahru, and B. G. Mitchell (1999), Estimation of Particulate Organic Carbon in the Ocean from Satellite Remote Sensing, Science, *285*(5425), 239-242. doi:10.1126/science.285.5425.239

Stramski, D., et al. (2008), Relationships between the surface concentration of particulate organic carbon and optical properties in the eastern South Pacific and eastern Atlantic Oceans, Biogeosciences, *5*(1), 171-201. doi:10.5194/bg-5-171-2008

Sullivan, J. M., and M. S. Twardowski (2009), Angular shape of the oceanic particulate volume scattering function in the backward direction, Appl. Opt., *48*(35), 6811-6819. doi:10.1364/ao.48.006811

Werdell, P. J., et al. (2013), Generalized ocean color inversion model for retrieving marine inherent optical properties, Appl. Opt., *52*(10), 2019-2037. doi:10.1364/AO.52.002019

Zhang, X., E. Boss, and D. J. Gray (2014), Significance of scattering by oceanic particles at angles around 120 degree, Opt. Express, *22*(25), 31329-31336. doi:10.1364/OE.22.031329

Figures

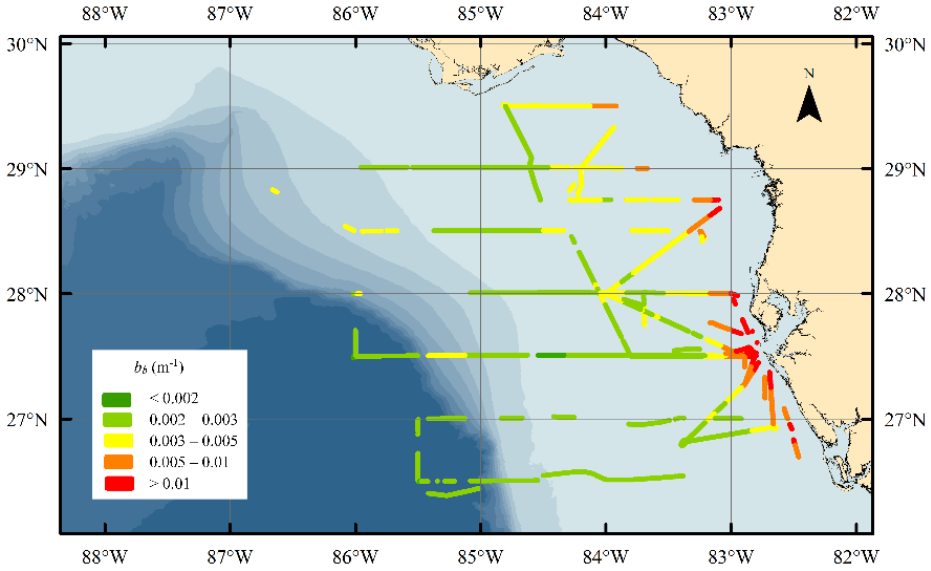

Figure 1. Map of lidar shots color coded by the value of satellite backscattering coefficient, b_b. Background colors indicate water depth with changes at 200, 400, 600, 800, 1000, 1200, 1500, 2000, and 3000 m. Gaps in flight tracks are because of gaps in satellite coverage or non-uniformity in the lidar profile.

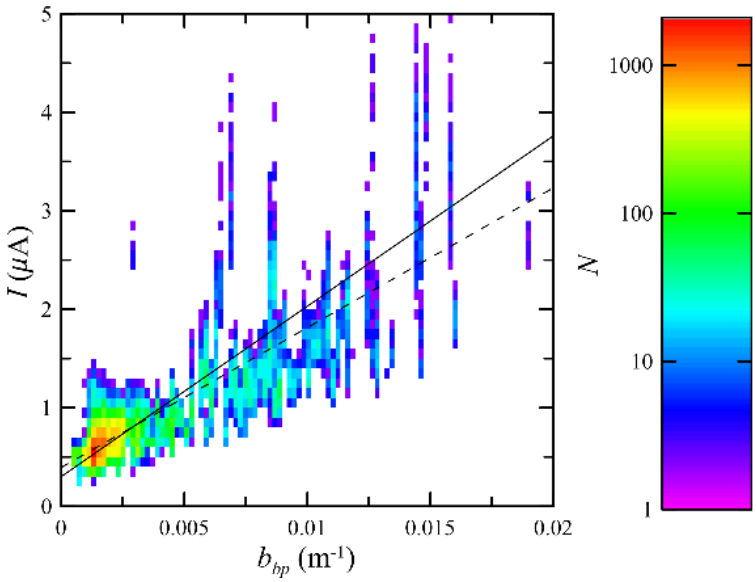

Figure 2. Histogram plot of lidar signal current, I, as a function of MODIS particulate backscatter coefficient, b_{bp}, with the number of samples in each bin denoted by color according to the color bar at the right. The ordinary regression is plotted as a dashed line. The reduced major axis regression as a solid line.